ELSEVIER

Remote Sensing of Environment 76 (2001) 33–48

Remote Sensing of Environment

www.elsevier.com/locate/rse

Dual-excitation FLIDAR for the estimation of epidermal UV absorption in leaves and canopies

A. Ounis*, Z.G. Cerovic, J.M. Briantais, I. Moya

Groupe Photosynthèse et Télédétection, LURE/CNRS, Bât 203, Centre Universitaire Paris-Sud, B.P. 34, 91898 Orsay cedex, France

Received 10 March 2000; accepted 19 September 2000

Abstract

A new FLIDAR was designed for remote quantitative assessment of epidermal UV absorption of leaves and canopies from chlorophyll (Chl) fluorescence (ChlF) measurements. The dual-excitation fluorescence light detection and ranging (DE-FLIDAR) performs a dual excitation of the Chl present in leaves, in the UV (355 nm) and visible (532 nm) part of the spectrum, the latter being used as a reference excitation not absorbed by the epidermis. Therefore, the epidermal UV absorption of vegetation can be estimated from the Chl fluorescence excitation ratio (FER), ΦF(532)/ΦF(355). Thanks to the alternated excitation by the DE-FLIDAR, the FER is immune to natural conditions in field, such as light-induced variable ChlF and leaf movement (variation of the angle of excitation). The DE-FLIDAR was used to investigate the presence of UV-absorbing compounds in individual leaves and canopies of different plant species, tobacco, pea, barley and wheat. The FER was much larger in outdoor-grown plants, indicating an accumulation of UV-absorbing compounds. We also analysed the epidermal UV absorption of the adaxial and abaxial side of tobacco leaves of different age. The logarithm of the FER showed a good agreement with the absorbance of methanolic extracts obtained from the same leaves. The presented DE-FLIDAR can perform up to three simultaneous fluorescence measurements; therefore, we could compare blue fluorescence (BR) to the epidermal UV absorption. In addition, a dual ratio, the red fluorescence (RF) to far-red fluorescence (FRF) emission ratio, excited at 355 and 532 nm, was shown to be linearly dependent on the Chl content. A mathematical model of leaf absorption and fluorescence, based on the Beer–Lambert's law, was developed to describe and analyse the fluorescence signatures obtained with the DE-FLIDAR.

1. Introduction

Laser-induced fluorescence (LIF) is used as a non-destructive and non-intrusive probe of plant leaf status. This technique has also become a sensitive and specific tool for the fluorescence remote sensing (fluorosensing) of vegetation. Under UV excitation, leaves emit blue fluorescence (BF), green fluorescence (GF), red fluorescence (RF), and far-red fluorescence (FRF), with maxima around 450, 530, 685, and 735 nm, respectively. RF and FRF emanate solely from chlorophyll (Chl), whereas BF and GF have multiple origins (Cerovic et al., 1999). UV-induced fluorescence can provide important information for plant ecophysiology and agronomy, like plant identification, monitoring of plant growth and development, mineral deficiency and presence of other stresses (for recent reviews, see Buschmann & Lichtenthaler, 1998; Cerovic et al., 1999).

Specific LIDARs (light detection and ranging) were developed for outdoor vegetation fluorosensing (Anderson et al., 1994; Cecchi et al., 1994; Chekalyuk & Gorbunov, 1995; Goulas et al., 1994; Günther et al., 1991; Hoge et al., 1983; Rosema et al., 1988). The main limitation of fluorescence LIDARs (FLIDARs) in remote sensing applications is that they measure amplitude signals, which depend on atmospheric transmission and distance. This problem can be overcome by performing simultaneous measurement of fluorescence emission, and by using fluorescence ratios as signatures (Cecchi et al., 1994; Günther et al., 1991; Lichtenthaler & Rinderle, 1988). On the other hand, fluorescence emission ratios (BF/RF or BF/FRF) present a limitation because they depend on two variables, which can vary independently, leading to ambiguous interpreta-

Abbreviations: BF, blue fluorescence; Chl, chlorophyll; ChlF, chlorophyll fluorescence; DE-FLIDAR, dual-excitation fluorescence LIDAR; ΦF, apparent fluorescence yield; FER, fluorescence excitation ratio "ΦF(532)/ΦF(355)"; FRF, far-red fluorescence; GF, green fluorescence; GR, green reflectance; LIDAR, light detection and ranging; PAR, photosynthetically active radiation; PPFD, photosynthetic photon flux density; RF, red fluorescence; S/N, signal-to-noise ratio; UVR, UV reflectance

* Corresponding author. Tel.: +33-1-64-46-82-08; fax: +33-1-64-46-80-07.

E-mail address: ounis@lure.u-psud.fr (A. Ounis).

0034-4257/00/$ – see front matter
PII: S0034-4257(00)00190-5

tion. Another alternative is to use fluorescence lifetime rather than the amplitude (Cerovic et al., 1996). Presently, the major limitation for the use of lifetime as signature is a more complex and more expensive instrumentation (Moya et al., 1995).

For example, LIF studies on the effects of UV radiation on plants reported an increase in the BF/ChlF ratio (BF/RF or BF/FRF) (Edner et al., 1994; Middleton et al., 1996; Sandhu et al., 1997; Schweiger et al., 1996; Stober & Lichtenthaler, 1993). UVB (280–320 nm) radiation is known to reduce the growth rate and photosynthesis and to affect flowering and reproduction (Caldwell, 1971; Caldwell et al., 1998; Gonzalez et al., 1996; Teramura & Sullivan, 1994; Tevini & Teramura, 1989), but the exposure to UVB radiation also induces an accumulation of phenolic compounds in the vacuoles and cell walls of leaf epidermis and in the cuticle (Caldwell et al., 1983; Cerovic et al., 1999; Schnitzler et al., 1996; Tevini & Teramura, 1989). These compounds are mainly flavonoids and hydroxycinnamic acid derivatives that strongly absorb UVB and UVA (320–400 nm) radiation and, then, can effectively screen the mesophyll from UV radiation. Therefore, the reported increase in the BF/ChlF ratio can be due to an accumulation of these compounds with high UV absorptivity. This screening effect of the epidermis on UV-induced Chl fluorescence (ChlF) was often noted in the literature (cf. Buschmann & Lichtenthaler, 1998; Cerovic et al., 1999), but the UV-induced ChlF was only rarely used to actually estimate epidermal absorption (see for e.g. Cerovic et al., 1993; Sheahan, 1996), until Bilger et al. proposed the use of the comparison between UV-induced and blue-green-induced ChlF as a nondestructive method to estimate the epidermal UV absorption (Bilger et al., 1997).

The UV absorption by leaf epidermis was initially demonstrated and analysed using epidermal peels (Caldwell et al., 1983; Gausman et al., 1975; Lautenschlager-Fleury, 1955). Later, fibre-optic microprobes introduced into intact leaves were used to determine the amount of UV radiation reaching the mesophyll (Bornman & Vogelmann, 1988; Cui et al., 1991; Day et al., 1994). Both of these established techniques for determining epidermal UV absorption showed that the adaxial epidermis of bifacial leaves is the major barrier for UV radiation, i.e. it is responsible for the major part of UV absorption of the leaf.

In this paper, we present a new FLIDAR instrument for the estimation of this epidermal UV absorption of leaves and canopies, based on dual excitation of Chl. The dual-excitation fluorescence light detection and ranging (DE-FLIDAR) uses 355 and 532 nm radiation from a frequency-tripled Nd:YAG laser for UV and visible excitation, the latter being used as a reference excitation. Therefore, the epidermal UV absorption of vegetation is estimated from the Chl fluorescence excitation ratio (FER), "ΦF(532)/ΦF(355)". A mathematical model, based on the Beer–Lambert's law, was also developed to describe how leaf epidermal UV absorption can be deduced quantitatively from dual ChlF measurement.

2. Material, methods and instrumentation

2.1. The source unit of the DE-FLIDAR

The DE-FLIDAR is built around a Q-switched flash lamp-pumped Nd:YAG laser, of 500 mJ per pulse (class IV) (Quanta–Ray, model CGR-170, Spectra-Physics, Orsay, France). A diagram of the DE-FLIDAR is shown in Fig. 1. The laser is operating at 50 Hz and producing 1064-nm radiation, which is then frequency-doubled (2ω) and tripled (3ω) to give 532- and 355-nm radiation.

In order to favour UV against green excitation, the 355-nm beam is separated first, with two dichroic mirrors (DMs) (0441-6080, Spectra-Physics). Then, the 532-nm beam is separated with a second pair of DMs (0441-6070, Spectra-Physics). The residual 1064-nm light is trapped in a beam dump (BD) (BD-5, Spectra-Physics). The resulting excitation beams have the following characteristics: at 355 nm, maximum energy per pulse 90 mJ, duration 4–6 ns (FWHM); at 532 nm, maximum energy per pulse 100 mJ, duration 5–7 ns (FWHM); pulse-to-pulse energy stability typically 20%; beam divergence less than 0.5 mrad and diameter less than 10 mm, for both beams. For greatest spectral purity, we added for each beam an isocel dispersive quartz prism (J. Fichou, Fresnes, France). High reflectivity mirrors (M) (16MFB133 and 16MFB153, for 355 and 532 nm, respectively; Melles Griot, Magny les hameaux, France) are used to redirect the beams (Fig. 1).

As the epidermal UV absorption of leaves can vary substantially (see below), it is advantageous to adjust the energy of the UV beam and the green beam independently, and to maintain the same intensity of the ChlF signal. In the DE-FLIDAR, the energy of each beam can be adjusted outside the laser cavity, by taking advantage of their linear polarisation. The insertion of a half-wave retardation plate (Plate) (02WRQ025, Melles Griot) and a polarising beamsplitter (P1 or P2) in the beam path permitted us to adjust continuously the output beam irradiance by suitably rotating the half-wave plate. For the 532-nm beam, we used a Glan laser polarising prism (P1) (03PGL303/A, Melles Griot), and for the 355 nm beam, we used a plate polariser (P2) at Brewster's angle (16PPQ025, Melles Griot), in order to avoid any deterioration of the polariser by UV radiation. The retardation plates are rotated by two step motors (82 971 002, Crouzet, Valence, France) (not shown), and the residual reflected beams are trapped into beam dumps (BDs) (BT 510/M, Thorlabs, NJ, USA).

Due to type I phase-matching in the SHG and THG, the second and third harmonics have perpendicular polarisation. Therefore, to avoid any potential differences in interaction of the two beams with the surface of leaves, a half-wave retardation plate (02WRQ025/355, Melles Griot) is inserted to rotate the UV beam to a vertical polarisation (the polarisation of the green beam).

Although the laser operates continuously at 50 Hz, the effective excitation repetition rate of the present DE-FLI-

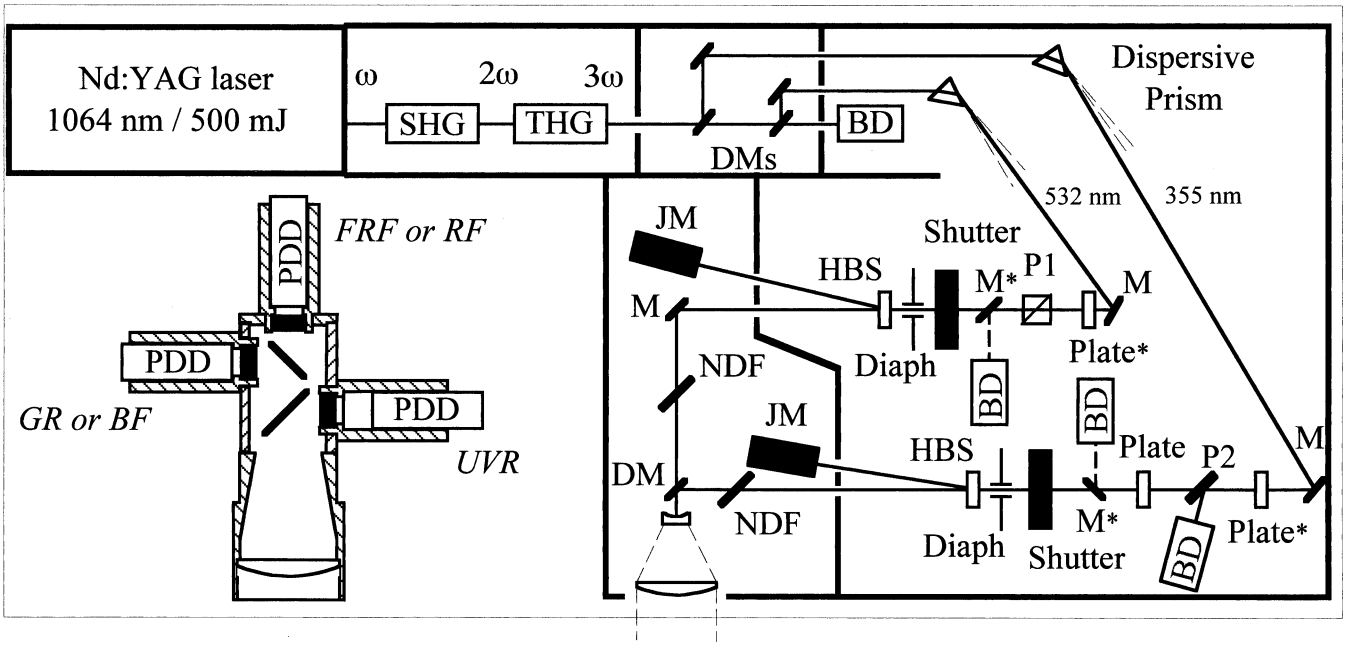

Fig. 1. Schematic diagram of the DE-FLIDAR. SHG: second harmonic generation; THG third harmonic generation; (*) rotated by a step motor. For a detailed description, see Material, methods and instrumentation.

DAR can be set only between 0.2 and 2 Hz, by using a combination of a moving mirror and a shutter, for each beam. A high reflectivity mirror (M*), mounted on a lever arm of a step motor (650 R726, Sonceboz, MDP, Miribel, France) and a rapid electromechanical shutter (Uniblitz, VS25S 2 ZM 0, Vincent Associates, Rochester, USA) are synchronised with the Q-switch synchro-output of the laser, and controlled, by a proprietary electronic circuit. This device, therefore, generates an alternated excitation at 532 and 355 nm with 500 ms delay time between beams at a variable repetition rate (1 Hz for the present study). The mirrors mounted on the step motors are not rapid enough to select only one pulse. They are used to protect the rapid diaphragm shutter from the high energy of the laser pulses. A beam dump (BD) (BD-5, Spectra-Physics) is used to trap the unused reflected pulses. With the present laser, the excitation rate can be increased to a maximum of 25 Hz.

Each shutter is followed by an iris diaphragm (Diaph), used to obtain an identical laser spot on the target for both excitations, and then followed by a holographic beam sampler (HBS) (HBS-532-100-1C-10, Gentec, Sainte-Foy, Quebec). The quartz HBS is actually a transmitting diffraction gratings, from which we use the first order to sample the pulse energy. The first-order diffraction angle at 532 nm is 10°, with a sampling ratio of 1.06%. At 355 nm, the angle is 6.6°, with a sampling ratio of 2.25%. The first-order diffracted radiation is then measured by a pyroelectric joulemeter (JM) (ED 200, Gentec). For each joulemeter, a differential amplifier based on an operational amplifier (OP-27, Analog Devices, Radiospares, Beauvais, France) was added. Thanks to this amplifier, only fast signals corresponding to laser pulses are amplified. Hence, any temperature and vibration dependencies are eliminated. The output signal from each amplifier is sampled by a sample-and-hold circuit (AD585, Analog Devices) synchronised to the exciting laser pulses via two TTL monostable multivibrators (SN74LS221N, Motorola, Radiospares). Additional neutral density filters (NDFs) (ARIES, Chatillon, France) are used when necessary (for leaves of high epidermal UV transmittance).

The two monochromatic light beams are finally combined in front of the output beam expander by a DM at 45° (16HSB105, Melles Griot). The beam expander consists of a planoconcave quartz lens (01LQS003, 25 mm diameter, 50 mm focal length, Melles Griot) and a planoconvex quartz lens (01LQF116, 50 mm diameter, 100 mm focal length, Melles Griot). For the present study, the DE-FLIDAR was adjusted to monitor the samples at 3.5 m, with a beam irradiating 190 cm^2 of the target area.

We used Rhodamine B on solid support as a photon counter to calibrate the measurements and to correct for optical losses downstream of the Joulemeter energy measurements.

2.2. The detection unit of the DE-FLIDAR

The DE-FLIDAR has an independent detector unit which performs three simultaneous measurements: UV reflectance (UVR), green reflectance (GR) (or BF) and FRF (or RF). Furthermore, by changing the DMs, simultaneous measurement of RF, FRF and BF is possible. Light from the target is received by a f/2.6 lens with 77-mm entrance aperture (Planoconvex lens, 01LPX279, in BK7, Melles Griot), which limits the field of view of the DE-FLIDAR detection

to the area excited by the laser beams. The incoming light is split into different wavelength bands by two DMs: first an UV mirror, at 45° (Balzers, Zaventem, Belgium), followed by a blue mirror, at 45° (DC blue, Balzers). Great care was taken to the problem of achieving identical optical conditions for each detector and also to avoid stray light.

The combination of the filters in front of detectors was as follows (see Fig. 2): for UVR, a UV transmitting filter (DUG11, Schott, Clichy, France); for FRF, a long-pass filter (KV550, Schott) and a 3-mm-thick red glass filter (RGN9, Schott); for RF, a long-pass filter (KV550, Schott) and a red interference filter (682DF22EM, Omega, Brattleboro, USA); for GR, a UV-blocking filter (KV408, Schott) and a green interference filter (532FS03-25, ARIES); for BF, a UV-blocking filter (KV408, Schott) and a blue interference filter (450WB80, Omega). Furthermore, a set of neutral density filters, from Omega, was used when necessary to reduce the signal amplitude.

The three-photodiode detectors (PDDs) are identical. They consist of a fast PIN photodiode (S3590-01, Hamamatsu, Massy, France) followed by a differential amplifier, which make them insensitive to continuous light. The differential amplifier is built on the same feedback principle as described in Cerovic et al. (1993) by using an integrating amplifier (OP27, Analog Devices) fed back to an operational amplifier (OP37, Analog Devices).

Stabilised signals from the photodiode detectors and the joulemeters are sampled by a data acquisition card (410 series, 16 inputs, bipolar 12 bits, Transera, Provo, UT) on board of a personal computer. Signals from the photodiode detectors are divided by the energy level, obtained from the joulemeters, in order to correct for the laser energy fluctuations (cf. Fig. 5). A proprietary program allows an online control of the experiment and display of measured signals.

2.3. Preparation of Rhodamine B on solid support

Pieces of polythene backed absorbing paper (20 × 20 cm, Benchkote plus, Whatman, Maidstone, UK) were soaked in an ethanolic solution of 12 g l^{-1} of Rhodamine B (Fluka, Saint-Quentin-Yvelines, France). Once dry, the paper support retained approximately 1 mg cm^{-2} of Rhodamine B. Immediately prior to use, the Rhodamine B on solid support was humidified with spectroscopic grade pure ethanol.

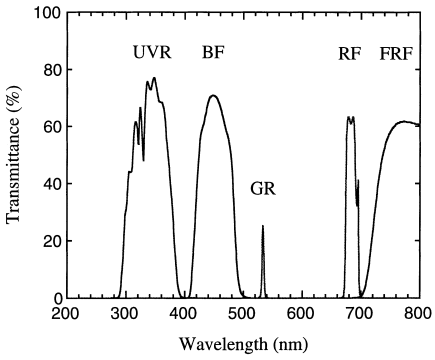

Fig. 2. Transmission spectra of the filter combinations used to protect the detectors and to define the spectral characteristics of fluorescence and reflectance signals. UVR: UV reflectance; GR: green reflectance; BF: blue fluorescence; FRF: far-red fluorescence; RF: red fluorescence.

2.4. Plant material

Plants were grown either in a growth cabinet (Sanyo, SGC970PPXF, Elancourt, France), or outdoors in Orsay, France (02°11′ longitude East, 48°41′ latitude North) in July 1999. Tobacco (*Nicotiana tabacum*, cv Burley) was grown in soil, and all other species, pea (*Pisum sativum* L., var. Petit Provençal), barley (*Hordeum vulgare*, cv Nevada) and wheat (*Triticum aestivum*, cv Lloyd) in pure wet vermiculite. Vermiculite trays were 40 cm long, 30 cm wide (0.12 m^2) and contained 1000 (230 g), 2000 (95 g) or 1000 (50 g) seeds of pea, barley or wheat, respectively. Vermiculite was maintained humid by regular watering with a nutrient solution equivalent to 5 × Hoagland (Hydrokani C_2, 5/1000 diluted, Hydro Agri, Neuilly sur Seine, France). The growth cabinet had a diurnal cycle of 16 h light (maximum photosynthetic photon flux density (PPFD) 1000 μmol photons m^{-2} s^{-1}, maximal temperature 24 °C, 60% minimum relative humidity) and 8 h dark (minimum temperature 18°C, 80% maximum relative humidity).

2.5. Preparation of thylakoids on solid support

Thylakoids were obtained from intact isolated pea chloroplast isolated from young pea shoots (10 days old) as described in Cerovic and Plesnicar (1984). Intact chloroplast were hypotonically disrupted by dilution in a hypotonic medium comprising: 13.2 mM sorbitol, 2 mM HEPES/KOH, pH 7.9, 0.4 mM KCl, 0.04 mM EDTA, 3 mM dithiothreitol, 5 mM $MgCl_2$. Thylakoids were recovered by centrifugation at 13 000 × *g* for 10 min, at 4°C (Eppendorf 5403 centrifuge, rotor 16F24-11, Vélizy, France). The pellets were resuspended in an isotonic medium comprising: 0.33 M sorbitol, 50 mM HEPES/KOH, pH 7.9, 10 mM KCl, 1 mM EDTA, 1 mM $MgCl_2$, 1 mM $MnCl_2$. The concentration of total Chl was determined according to Bruinsma (1961). Thylakoids were then trapped on solid supports, as described for chloroplasts in Cerovic et al. (1987). In the present study, the cellulose filter supports were replaced by glass-fibre filter supports (Millipore prefilters, AP 40, Saint-Quentin-Yvelines, France) in order to avoid any UV-induced blue-green fluorescence of the support. The content of thylakoids per unit surface was precisely adjusted, and it ranged from 5 to 70 μg Chl cm^{-2}.

2.6. Preparation of leaf extracts and recording of absorption spectra

Tobacco leaves were sampled for pigment extraction using a cork borer with 2 cm^2 aperture (two samples per

leaf). Leaf samples were frozen, and then pigments extracted by heating for 30 min at 70°C in 12 ml of methanol. Absorbance of cooled extracts was measured on a HP 8453 diode-array spectrophotometer (Hewlett-Packard, Les Ulis, France) from 200 to 800 nm. Chl *a* and *b* contents were calculated using molar absorptivities and formulas from (Lichtenthaler, 1987). Knowing the spectra of pure Chl *a* and *b* in methanol (from 200 to 800 nm, Cerovic et al., 1999), and the Chl *a* to *b* ratio, their contributions to the absorption spectrum of total leaf extract could be calculated and subtracted. This yields the spectrum of other compounds present in the extract, including carotenoids and phenolics (Fig. 3). For comparative purposes, the distribution of total Chl content on the surface of tobacco leaves was also estimated, and the average calculated, using a portable Chl meter (SPAD-502, Minolta, Carrière-Sur-Seine, France) (cf. Fig. 8B).

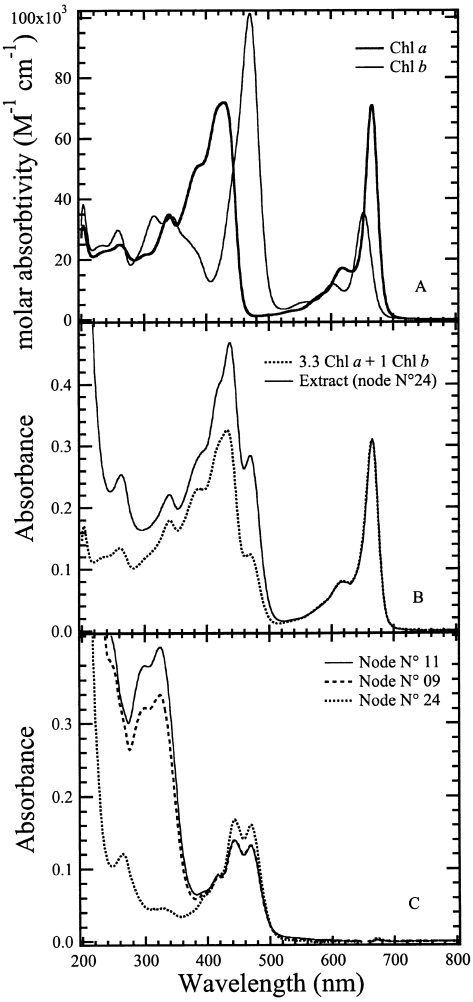

Fig. 3. Absorption spectra of pigments and extracts. (A) Absorption spectra of pure Chl *a* and Chl *b* in methanol. (B) Calculated absorption spectrum of 3.3 parts of Chl *a* and 1 part of Chl *b*, compared to the absorption spectrum of a methanolic extract of 2-cm^2 sample of tobacco leaf from node 24. The spectrum of the Chl mixture was normalised to the red maximum of the leaf extract. (C) Comparison of the absorption spectra of methanolic extracts from three leaves, nodes 9, 11 and 24 (the youngest), from which the contribution of Chls was subtracted.

3. Results and discussion

3.1. Theoretical consideration on the FER

Before presenting the results of the measurements obtained with the DE-FLIDAR, we would like to review the factors that can influence the fluorescence signatures obtained with this new LIDAR. For that purpose, we developed a model which describes the relationship that links the FER to the epidermal UV transmittance of leaves.

Let us consider a simplified leaf consisting of an epidermis with a transmittance $T(\lambda_{ex})$, and a mesophyll, which has only chloroplasts with a homogeneous Chl concentration c. The fluorescence emitted from the mesophyll is detected in front face and is assumed to be negligibly absorbed by the epidermis. In this model, we assume that light scattering, in the mesophyll, has a negligible effect, so only Beer–Lambert's law governs light propagation. Due to a partial overlapping of the fluorescence and the absorption spectrum of Chl, part of the fluorescence emission is reabsorbed, but we consider that the contribution of the reemitted fluorescence is negligible.

If an incident laser beam I_0, at wavelength λ_{ex}, reaches a leaf, the transmittance of the epidermis at that wavelength is defined by

$$T(\lambda_{ex}) = \frac{I_m(\lambda_{ex})}{I_0(\lambda_{ex})} \quad (1)$$

where $I_m(\lambda_{ex})$ is the light intensity of the laser at the mesophyll surface.

The intensity of the laser light inside the mesophyll, which reaches an infinitesimal layer dx after travelling the path x, is given by

$$I(x, \lambda_{ex}) = I_m(\lambda_{ex}) e^{-\alpha(\lambda_{ex})x} \quad (2)$$

where $\alpha(\lambda_{ex})$ is the absorptivity of the mesophyll at the laser excitation wavelength. The intensity of chlorophyll fluorescence (ChlF), $d\mathscr{F}_{\lambda_{ex}}(x,\lambda_{em})$, emitted by the same layer dx is the product of the fluorescence quantum yield η and the fraction of light absorbed by dx:

$$\begin{aligned} d\mathscr{F}_{\lambda_{ex}}(x, \lambda_{em}) &= -\eta\psi(\lambda_{em}) dI(x, \lambda_{ex}) \\ &= \eta\psi(\lambda_{em})\alpha(\lambda_{ex}) I(x, \lambda_{ex}) dx \end{aligned} \quad (3)$$

where $\psi(\lambda_{em})$ is the normalised spectral composition of Chl *a* fluorescence. The combination of Eqs. (2) and (3) leads to Eq. (4)

$$d\mathscr{F}_{\lambda_{ex}}(x, \lambda_{em}) = \eta\psi(\lambda_{em})\alpha(\lambda_{ex}) I_m(\lambda_{ex}) e^{-\alpha(\lambda_{ex})x} dx \quad (4)$$

The ChlF, which propagates opposite to the excitation, reaches the epidermis after crossing the same path

x in the mesophyll. Consequently, the contribution of the dx layer to the measured fluorescence is given by Eq. (5)

$$\begin{aligned} \mathrm{d}F_{\lambda_{ex}}(x,\lambda_{em}) &= \Omega \mathrm{d}\mathscr{F}_{\lambda_{ex}}(x,\lambda_{em})\mathrm{e}^{-\alpha(\lambda_{em})x} \\ &= \Omega\eta\psi(\lambda_{em})\alpha(\lambda_{ex})I_m(\lambda_{ex})\mathrm{e}^{-[\alpha(\lambda_{ex})+\alpha(\lambda_{em})]x}\mathrm{d}x \end{aligned} \tag{5}$$

where Ω depends on the collecting efficiency of the detector. As the same photodetector is used to measure the dual excited ChlF, Ω is invariable for both excitation wavelengths. By integrating this equation over the mesophyll thickness ℓ, we obtain the total measured fluorescence:

$$\begin{aligned} F_{\lambda_{ex}}(\lambda_{em}) = \Omega\eta\psi(\lambda_{em})I_m(\lambda_{ex})\frac{\alpha(\lambda_{ex})}{\alpha(\lambda_{ex})+\alpha(\lambda_{em})} \\ \times\left[1-\mathrm{e}^{-[\alpha(\lambda_{ex})+\alpha(\lambda_{em})]\ell}\right] \end{aligned} \tag{6}$$

On the other hand, the relationship between the absorptivity and the molar absorptivity (or molar extinction coefficient) is defined as

$$\alpha(\lambda) = \ln(10)\varepsilon(\lambda)c \tag{7}$$

Furthermore, the absorbance is defined as the product of the molar absorptivity, $\varepsilon(\lambda)$, at the specific wavelength, the molar concentration, c, and the path length, ℓ.

$$A(\lambda) = \varepsilon(\lambda)c\ell = \varepsilon(\lambda)C_{Chl} \tag{8}$$

where C_{Chl} is the Chl surface content in the mesophyll. Combining Eq. (6) with Eqs. (7) and (8), we obtain

$$\begin{aligned} F_{\lambda_{ex}}(\lambda_{em}) = \Omega\eta\psi(\lambda_{em})I_m(\lambda_{ex})\frac{\varepsilon(\lambda_{ex})}{\varepsilon(\lambda_{ex})+\varepsilon(\lambda_{em})} \\ \times\left[1-10^{-[\varepsilon(\lambda_{ex})+\varepsilon(\lambda_{em})]C_{Chl}}\right] \end{aligned} \tag{9}$$

Let us now consider the apparent fluorescence yield, which is defined by Eq. (10)

$$\Phi F(\lambda_{ex}) = \frac{F_{\lambda_{ex}}(\lambda_{em})}{I_0(\lambda_{ex})} \tag{10}$$

Applying Eq. (1) for both excitation wavelengths, at 355 and 532 nm, we obtain

$$\begin{aligned} \frac{\Phi F(355)}{\Phi F(532)} &= \frac{F_{355}(\lambda_{em})}{I_0(355)}\frac{I_0(532)}{F_{532}(\lambda_{em})} \\ &= \frac{T(355)}{T(532)}\frac{F_{355}(\lambda_{em})}{I_m(355)}\frac{I_m(532)}{F_{532}(\lambda_{em})} \end{aligned} \tag{11}$$

then, substituting Eq. (9) into Eq. (11), this yields Eq. (12)

$$\begin{aligned} \frac{\Phi F(355)}{\Phi F(532)} = \frac{T(355)}{T(532)}\frac{\varepsilon(355)}{\varepsilon(355)+\varepsilon(\lambda_{em})} \\ \times\frac{\varepsilon(532)+\varepsilon(\lambda_{em})}{\varepsilon(532)} \\ \times\frac{\left[1-10^{-[\varepsilon(355)+\varepsilon(\lambda_{em})]C_{Chg}}\right]}{\left[1-10^{-[\varepsilon(532)+\varepsilon(\lambda_{em})]C_{Chl}}\right]} \end{aligned} \tag{12}$$

Let us introduce the distortion function, $D(C_{Chl},\lambda_{em})$, defined by the relation below

$$\begin{aligned} D(C_{Chl},\lambda_{em}) = \frac{\varepsilon(532)}{\varepsilon(532)+\varepsilon(\lambda_{em})}\frac{\varepsilon(355)+\varepsilon(\lambda_{em})}{\varepsilon(355)} \\ \times\frac{\left[1-10^{-[\varepsilon(532)+\varepsilon(\lambda_{em})]C_{Chl}}\right]}{\left[1-10^{-[\varepsilon(355)+\varepsilon(\lambda_{em})]C_{Chl}}\right]} \end{aligned} \tag{13}$$

In the epidermis, the transmittance of UV-absorbing compounds, at 532 nm, is equal or close to 1, the FER becomes

$$\frac{\Phi F(355)}{\Phi F(532)} = T(355)\frac{1}{D(C_{Chl},\lambda_{em})} \tag{14}$$

The distortion function, $D(C_{Chl},\lambda_{em})$, defined by Eq. (13) has a simplified expression when ChlF is not reabsorbed. Hence, for λ_{em} above 730 nm, the distortion function becomes (Eq. (15))

$$D(C_{Chl},730) = \frac{1-10^{-\varepsilon(532)C_{Chl}}}{1-10^{-\varepsilon(355)C_{Chl}}} \tag{15}$$

The epidermal absorbance, at 355 nm, can also be written as

$$A(355) = \log\left(\frac{1}{T(355)}\right) \tag{16}$$

and by substituting Eq. (14) into Eq. (16), this yields Eq. (17)

$$\log\left[\frac{\Phi F(532)}{\Phi F(355)}\right] = A(355)+\log[D(C_{Chl},\lambda_{em})] \tag{17}$$

This shows that the FER, "ΦF(532)/ΦF(355)", in a logarithmic form, corresponds to the epidermal UV absorbance at 355 nm.

From the above, it can be concluded that for the excitation of Chl at two wavelengths of equal molar absorptivities, the logarithm of the FER is equal to UV-epidermal absorbance. When the absorptivities at the two wavelengths differ, the FER is still proportional to UV-epidermal absorption (the reciprocal of transmittance), but it has to be corrected for the distortion function, which depends on the Chl content of the leaf. Chl has very different absorptivities at the two wavelengths available for excitation with the DE-FLIDAR, therefore, the FER obtained has to be corrected for Chl content of the sample for quantitative estimation of UV-epidermal absorption (see below). Still, for leaves and canopies in which the Chl content does not vary much, the FER can be used without correction for comparative purposes. In addition, as will be seen later, this dependency on Chl content can actually be used to estimate nondestructively both the Chl content and the epidermal UV absorbance of leaves.

3.2. The effect of Chl content on the FER

To check the above-developed model, the FER was measured on pea thylakoids of known Chl content using the DE-FLIDAR. The thylakoids were layered on solid

supports under conditions that approximate the geometry and optical properties of Chl in leaf samples. The total surface of the sample was 37.5 cm^2. Thanks to the absence of any UV screening, the measured excitation ratio directly reflects the effect of Chl content corresponding to the distortion function (Fig. 4A). The excitation ratio measured using FRF emission, above 730 nm where ChlF is not reabsorbed, was compared to the excitation ratio measured using RF at 682 nm, which is strongly reabsorbed. As seen in Fig. 4A, there is a good agreement between the model and the experimental results. The best fit of the data was obtained with specific absorptivities at 355, 532 and 682 nm of 0.0482, 0.0166 and 0.0545 μg^{-1} cm^2, respectively, which were very close to those obtained previously on intact isolated chloroplasts (Cerovic, Langrand, Latouche, Morales, & Moya, 1998). For the FRF excitation ratio, there is a significant increase with a tendency to saturation above 70 $\mu g\ cm^{-2}$. With RF emission, even though the agreement is less good between the excitation ratio and the distortion function, both of them show a weak dependency on Chl content, with a relatively constant offset of about 0.5, above 20 $\mu g\ cm^{-2}$ (Fig. 4A). Actually, this offset corresponds to the proportional factor of the distortion function given by

$$D(C_{\mathrm{Chl}} > 20, 682) \approx \frac{\varepsilon(532)}{\varepsilon(532)+\varepsilon(682)} \frac{\varepsilon(355)+\varepsilon(682)}{\varepsilon(355)} = 0.53$$

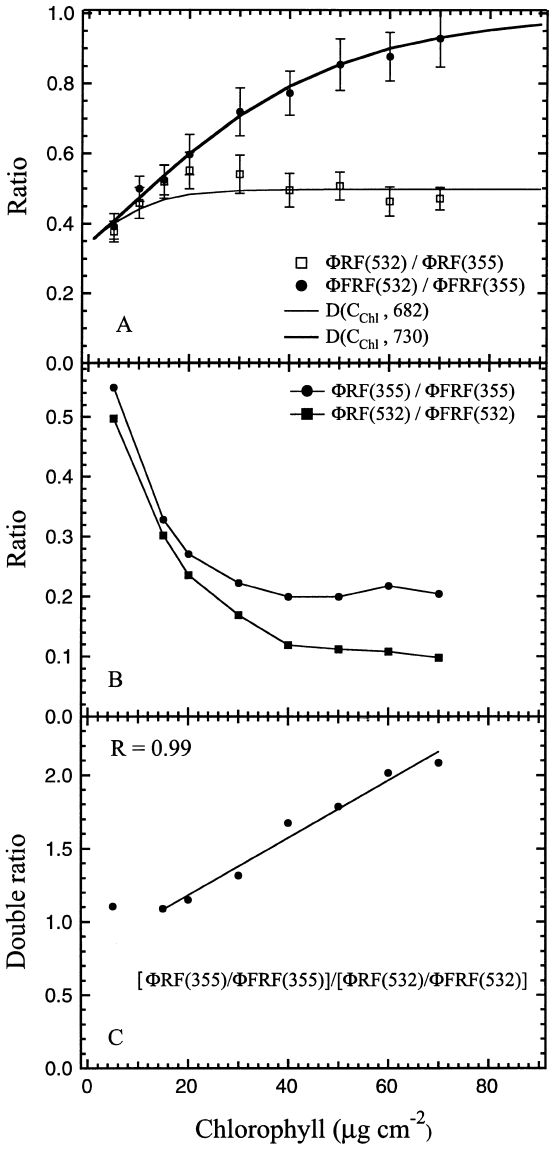

Fig. 4. Dependence of the FER on the Chl content, and estimation of the Chl content by the fluorescence double emission ratio. The excitation and emission ratios were measured using DE-FLIDAR on pea thylakoids layered on solid supports at different concentrations. The total surface of the sample was 37.5 cm^2. (A) The FER, "ΦFRF(532)/ΦFRF(355)" and "ΦRF(532)/ΦRF(355)", were measured above 730 nm and at 682 nm, respectively, and fitted by the distortion functions, "$D(C_{\mathrm{Chl}}, 730)$" and "$D(C_{\mathrm{Chl}}, 682)$". The error bars denote the standard deviation ($N = 170$). (B) The emission ratios, "ΦRF(355)/ΦFRF(355)" and "ΦRF(532)/ΦFRF(532)", excited at 355 and 532 nm, respectively, were measured for different Chl contents. (C) The dual fluorescence emission ratio, defined as "[ΦRF(355)/ΦFRF(355)]/[ΦRF(532)/ΦFRF(532)]", was linearly dependent on the Chl content. A linear fit gives a correlation coefficient of $R = .99$.

The relatively weak dependency on the Chl content, when the ChlF is measured in the red spectral range, can be explained by the reabsorption of the ChlF coming from deeper layers of the sample. Indeed, the 355-nm beam is absorbed within the first chloroplast layers due to the high absorptivity of Chl at this wavelength, whereas, the 532-nm beam penetrates deeper in the sample and can even be transmitted through when the Chl content is small.

It should be noted that the model showed a good agreement with experimental results on chloroplasts, even though it neglects the problem of scattering. Indeed, it is well known that the mesophyll of leaves scatters radiation to a large extent. Differential scattering of UV and green radiation might cause a difference in distribution of radiation in the epidermis and mesophyll and, therefore, a different distribution of Chl excitation. It is possible to take into account the effect of excitation and emission scattering in the mesophyll by using an extended Kubelka–Munk theory, where multiple elastic scattering is taken into consideration (Fukshansky & Kazarinova, 1980), or by using the effective optical path length due to diffuse propagation, which is longer than mesophyll thickness (Agati, Fusi, Mazzinghi, & diPaola, 1993). A model incorporating the Kubelka–Munk theory showed no substantial difference compared to the model described in this report (not shown), suggesting that any additional optical influence on FER at the leaf level can come from leaf structure, and not from scattering per se.

3.3. Estimation of the Chl content from the fluorescence emission ratios

The reabsorption phenomenon, described above, has already been exploited by Lichtenthaler et al. (for recent

reviews, see Buschmann & Lichtenthaler, 1998) to estimate Chl content of a leaf using ChlF. They used the emission RF/FRF ratio that decreases with increasing Chl content. The RF/FRF ratio can also be measured using the DE-FLIDAR. Fig. 4B shows the ΦRF/ΦFRF emission ratio, excited at 355 or 532 nm, measured on pea thylakoids on solid support for different Chl contents. As expected, when increasing the Chl content, due to the reabsorption of the RF emission, both ΦRF(355)/ΦFRF(355) and ΦRF(532)/ΦFRF(532) ratios show a decrease reaching a plateau, which corresponds to a saturation of the Chl absorption. Thanks to a smaller absorptivity of Chl in the green spectral region, the 532-nm excitation beam penetrates deeper in the leaf (Cui et al., 1991), and consequently, the green-induced ChlF emission ΦRF(532) is more attenuated than the UV-induced one. The ΦRF(532)/ΦFRF(532) ratio shows saturation at much larger Chl contents. Because both ΦRF(355)/ΦFRF(355) and ΦRF(532)/ΦFRF(532) ratios are governed by the same propagation laws, the dual emission ratio, defined as "[ΦRF(355)/ΦFRF(355)]/[ΦRF(532)/ΦFRF(532)]", is linearly dependent on the Chl content (Fig. 4C).

3.4. Signals characteristics

Fig. 5 illustrates and characterises the signals obtained by the DE-FLIDAR for fluorescence yields and ratios. In this particular experiment, the laser flash lamps were at about 80% of their total lifetime, therefore, the laser fluctuations were greater than the expected 20%. The pulse-to-pulse energy stability was 24% and 39% at 532 and 355 nm, respectively (Fig. 5A and C). The characteristics of the excitation beams for this experiment are summarised in Table 1. The calculated photon flux density (spot size of 190 cm^2) is weak enough for analysis at both wavelengths. In spite of relatively large energy fluctuation of both excitations, the apparent fluorescence yields, ΦFRF(532) and ΦFRF(355), have a relatively weak noise (Fig. 5E and F), thanks to a good correlation between signals from the photodiode detectors and the pyroelectric joulemeters. Generally, for laser fluctuations of 20%, the signal-to-noise ratio (S/N) of the measurements is much better. It should also be noted that the noise of the FER (Fig. 5G) contains the noise contribution of four signals.

In Table 2, we summarised different signal characteristics from experiments performed under two extreme conditions, on barley canopies grown indoors and outdoors. The laser and fluorescence signal fluctuations are evaluated both by the standard deviation and by the S/N. The UV excitation shows energy fluctuations greater than those of the green excitation, as expected, because the UV radiation is generated in the THG from the green one. In terms of S/N, the

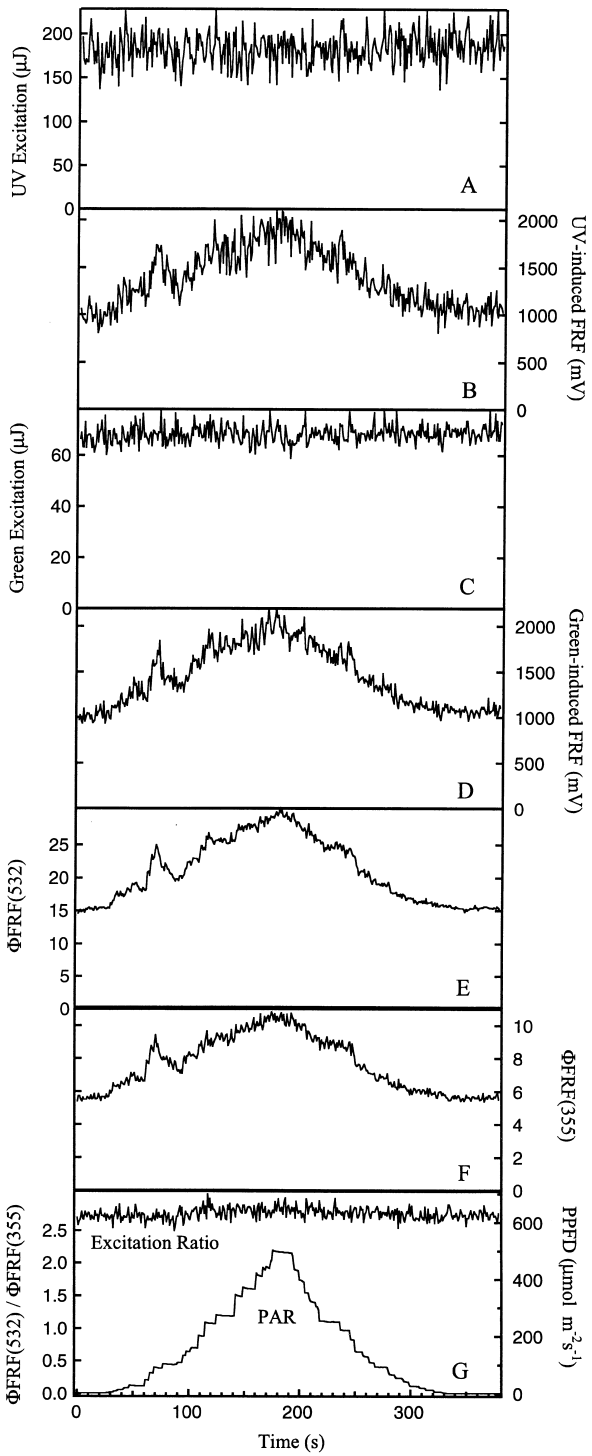

Fig. 5. Variation of fluorescence signals and FER during slowly induced changes in actinic light. Measurements were performed on the adaxial side of a tobacco leaf. Excitation at 355 and 532 nm was alternated with a delay time of 500 ms and a repetition rate of 1 Hz for each excitation. The leaf was first dark-adapted for more than 15 min. Variable ChlF was induced by white actinic light, whose PPFD was changed in small steps from darkness to 500 μmol m^{-2} s^{-1}. (A) Signal from the joulemeter that monitors UV excitation at 355 nm, (B) UV-induced FRF, (C) signal from the joulemeter that monitors green excitation at 532 nm and (D) green-induced FRF. The energy of the UV-excitation beam was set to induce the same ChlF level as the one induced by the green excitation. (E and F) Apparent FRF yields, ΦFRF(532) and ΦFRF(355), excited at 532 and 355 nm, respectively. (G) FRF excitation ratio (FER). No smoothing was applied at any time.

Table 1
Characteristics of the excitation beams of the DE-FLIDAR

	Average energy (μJ)	Irradiance (mW m^{-2})	Photon flux density (nmol m^{-2} s^{-1})	Pulse-to-pulse stability (%)
UV excitation	183	9.63	29	39
Green excitation	68	3.58	16	24

The photon flux densities were calculated for a spot size of 190 cm^2.

fluctuation was 1.6-fold greater for UV than for green excitation. However, a very similar S/N was obtained for outdoor and indoor conditions, both for fluorescence yields and final FERs. In these experiments, and in general with our DE-FLIDAR, the energy of the UV beam was set to induce the same ChlF level as the one induced by the green beam. This is why the energy of the UV beam was much higher than the green one. Therefore, even though the final FER for the outdoor canopy is much larger than the one grown indoors (sixfold), the S/N is nearly the same and reasonably good.

3.5. Photoinduced variable ChlF

If we want to use ChlF as a measure of epidermal UV absorbance, its yield has either to be constant or the measurement of fluorescence excited at the two wavelengths has to be completed before the yield has changed. Under natural conditions, this might be very difficult to achieve considering the variability of solar illumination. We therefore tested the effect of slow and rapid changes in ChlF yield on the measured FER obtained by our DE-FLIDAR.

Table 2
Comparison of signal characteristics obtained by the DE-FLIDAR under two extreme conditions

	Signals	Indoors	Outdoors
Green excitation	Average energy (μJ)	46.30	52.02
	S.D. (μJ)	3.43	3.07
	S/N	13.49	16.97
ΦFRF(532)	Average FRF yield (mV/μJ)	118.31	54.01
	S.D. (mV/μJ)	2.55	1.12
	S/N	46.49	48.19
UV excitation	Average energy (μJ)	189.53	850.44
	S.D. (μJ)	21.73	79.25
	S/N	8.72	10.73
ΦFRF(355)	Average FRF yield (mV/μJ)	31.45	2.37
	S.D. (mV/μJ)	0.48	0.03
	S/N	66.00	76.51
Fluorescence excitation ratio	Average ratio	3.76	22.84
	S.D.	0.09	0.51
	S/N	40.85	44.84

The "indoors" column corresponds to the minimum FER measured on a barley canopy, grown in a growth cabinet. The "outdoors" column corresponds to the maximum FER measured on a barley canopy, grown outdoors, in July. The laser fluctuations are evaluated by the standard deviation and also by the S/N.

A tobacco leaf was dark adapted for more than 15 min, then FRF was measured with the DE-FLIDAR on the adaxial side of the leaf, excited at 355 and 532 nm. The energy of the UV-excitation beam was set to induce the same FRF level as the one induced by the green excitation (Fig. 5B and D). Changes in the yield of FRF where then induced with white actinic light, by varying in small steps its PPFD from darkness to 500 μmol m^{-2} s^{-1}. Even though the apparent fluorescence yield ΦFRF(355) was smaller than the yield ΦFRF(532) due to epidermal UV absorption (Fig. 5E and F), they changed in parallel. Hence, as shown in Fig. 5G, in spite of changes in ChlF yield, the FER remained quite constant during the whole experiment. The average FER was 2.76 with a standard deviation of 0.09, which gives a S/N of 30.67. Similar results showing the insensitivity of FER to slow variations of actinic light have been obtained on barley and pea canopies (data not shown).

Fig. 6 illustrates the effect of fast changes in actinic light intensity that induces large changes in ChlF yield

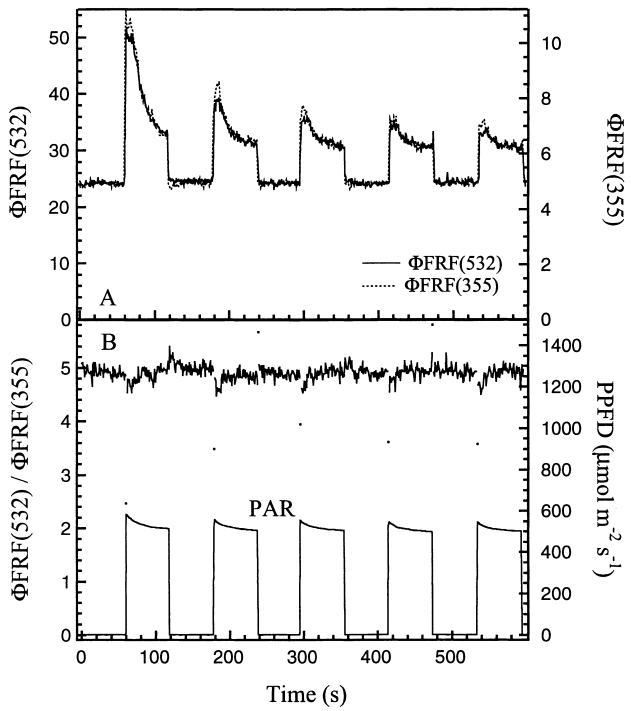

Fig. 6. Effects of large changes in ChlF yield on FER. (A) Dual FRF kinetics, induced at 355 and 532 nm, on a dark-adapted barley canopy, illuminated with a white actinic light (PPFD 500 μmol m^{-2} s^{-1}) by alternating light and dark periods every minute. The UV exciting energy was set to induce the same ChlF level as that induced by the green excitation. Excitation at 355 and 532 nm was alternated with a delay time of 500 ms and a repetition rate of 1 Hz for each excitation. The barley canopy was exposed at an angle of 45° to the excitation beams and to the detector. The UV-induced fluorescence and green-induced fluorescence were normalised to Fo. (B) Calculated FER changes during actinic light transitions. The average value of the FER in the dark-adapted region was 4.921 ± 0.093, whereas the average value for the whole experiment was 4.894 ± 0.196. This leads to a relative measurement error for FER of 0.5%.

(photosynthetic induction). A dark-adapted barley canopy was illuminated with a white actinic light (PPFD 500 μmol m^{-2} s^{-1}) intermittently by alternating light and dark periods every minute. The ChlF was measured in the far-red spectral range (FRF). The UV-induced FRF and green-induced FRF were normalised to the Fo level and plotted in Fig. 6A. In spite of the heterogeneity in the canopy, the variable ChlF behaved like in a single leaf. The whole canopy seemed to be synchronised by the actinic light.

The actual dual sampling rate of 1 Hz of our DE-FLIDAR, with 500 ms delay time, was not sufficient to sample very rapid dark–light induction kinetics, therefore, differences could be seen during the rapid transients when comparing UV and green excitation or with FER trace. The UV-induced fluorescence shows a larger increase in yield during the beginning of the inductions. Similar results were also obtained on pea canopies (data not shown). These differences in kinetics can be attributed to the penetration depth of the excitations that is larger for 532 nm than 355 nm excitation (Cui et al., 1991; Vogelmann, 1993) or to different spectral sensitivity of variable ChlF due to different excitation of PSII and PSI pigment matrices (Percival & Baker, 1985). Despite these small changes induced by rapid light transitions, the FRF excitation ratio remained remarkably constant during the experiment (Fig. 6B). The average value of the FER, in the dark-adapted period, was 4.921 ± 0.093, compared to the total average value of 4.894 ± 0.196 for the whole experiment. Therefore, drastic light transitions induced a relative error in the measurement of the FER of only 0.5%. Similar results were also obtained with tobacco leaves and pea canopy (data not shown). Hence, this confirms that the FER, ΦFRF(532)/ΦFRF(355), when monitored by the DE-FLIDAR, is basically insensitive to photoinduced changes in ChlF yield.

3.6. Dependency of the FER on the angle of incidence of the excitation beam

Another frequent problem for fluorescence remote sensing is variation of the apparent fluorescence yield with the angle of incidence of the excitation beam. In order to check whether this potential effect can influence the FER, a tobacco leaf was exposed at different incident angles, with the excitation beams and the detector at fixed position. Fig. 7 shows that ChlFs, excited both at 355 and 532 nm, exhibit a maximum yield for a normal incidence. Still, the FER remained invariable for all incidence angles.

3.7. Epidermal UV absorption of tobacco leaves

We can now use the DE-FLIDAR to analyse the variability of epidermal UV absorbance among plant species and during plant development; but first, we will compare absorbances obtained from fluorescence measurement to absorbances of leaf extracts.

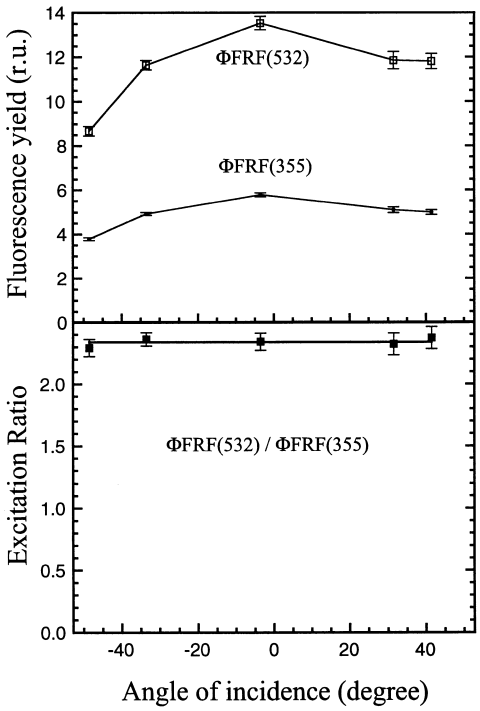

Fig. 7. Dependence of the FER on the angle of incidence. FRF, excited at 355 and 532 nm, and FER were measured on a tobacco leaf. The leaf was exposed at different angles of incidence, while the excitation beams and the detector remained at the same position. The error bars denote the standard deviation ($N = 170$).

In Fig. 8A, the FER, ΦFRF(532)/ΦFRF(355), is shown for tobacco leaves grown indoors, in a growth cabinet. The FER was measured on adaxial and abaxial leaf sides at different stages of development, from the older leaf (node No. 8) to the youngest one (node No. 24) on the same plant. As reported for other plant species (Bilger et al., 1997), the adaxial side had a higher FER (i.e. higher UV absorption) than the abaxial sides in all leaves. This difference is attributed to the light exposure of plants, which is much higher for the adaxial leaf side. Furthermore, the FER decreases from aged leaves to younger ones for both leaf sides. The FER of the abaxial side of several younger leaves remains at an almost constant level below 1.

Chromatographic analysis of tobacco leaf extracts revealed the presence of phenolic compounds like quercetin and kaempferol (flavonols), caffeic acid (a hydroxycinnamic acid) and scopoletin (a coumarin) (Bate-Smith, 1962). Esters of caffeic acid, like chlorogenic acid (3-caffeoylquinic acid) and its isomers, have been repeatedly reported as major UV-absorbing compound in tobacco under stress (del Moral, 1972; Koeppe et al., 1969; Loche & Chouteau, 1963). Takahama also showed that chlorogenic acid accumulated during leaf ageing (Takahama, 1998). Absorption spectra of methanolic extract of old tobacco leaves (Fig. 3) indicate that esters of caffeic acid could be the main

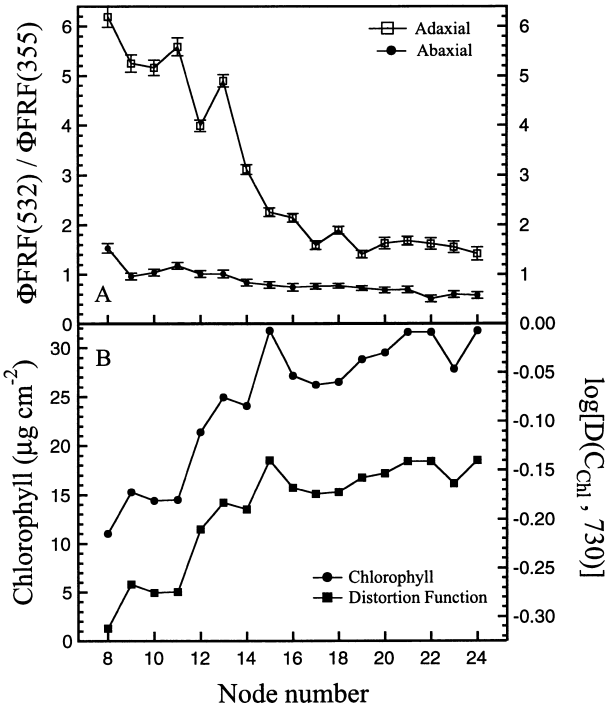

Fig. 8. FER of adaxial and abaxial sides of tobacco leaves at different nodes on the stem. Tobacco was grown in a growth cabinet. (A) The FER, ΦFRF(532)/ΦFRF(355), was measured on adaxial and abaxial sides of the leaves coming from different nodes of the same plant, the oldest leaf (node No. 8) and the youngest leaf (node No. 24). The error bars denote the standard deviation ($N = 170$). (B) The Chl content of leaves was estimated using a portable Chl meter (SPAD-502, Minolta). Each point is an average value measured at several positions on the leaf. The distortion function (for $\lambda > 730$ nm) was calculated for each leaf Chl contents and presented in the bottom part of the figure.

component responsible for the epidermal UV absorption. Indeed, the spectra have a maximum of absorption at 326 nm with a shoulder at around 298 nm, which correspond to the absorption spectrum of pure chlorogenic acid (not shown) (see also Lichtenthaler et al., 1990; Takahama, 1998). Other esters of cinnamic acids cannot be excluded at this point, because of the similarity of their absorption spectra. Still, it is reasonable to say that the increased FER in aged leaves corresponds to an accumulation of chlorogenic acid.

As to the variations of the FER seen on adjacent leaves (Figs. 8 and 9, cf. leaf nodes 11 and 12, for example), which are matched by variations of the corresponding extract absorbances, they can be the consequence of the different illumination received by adjacent leaves (known to be on opposite sides of the stem in tobacco). The weak value of the FER of abaxial side reflects the weaker epidermal UV absorption. The absolute value of the ratio is smaller than 1 because of the smaller efficiency of ChlF excitation at 532 nm than at 355 nm (spectra not shown). To correct for the effect of Chl content on FER, we measured the Chl content for each tobacco leaf, and calculated the distortion function (for $\lambda > 730$ nm) for each leaf (Fig. 8B). The latter was used in Fig. 9, where the logarithm of the FER, which should be equal to the epidermal UV absorbance at 355 nm, was compared to absorbances of extracts obtained from leaves at different nodes along the tobacco stem. As

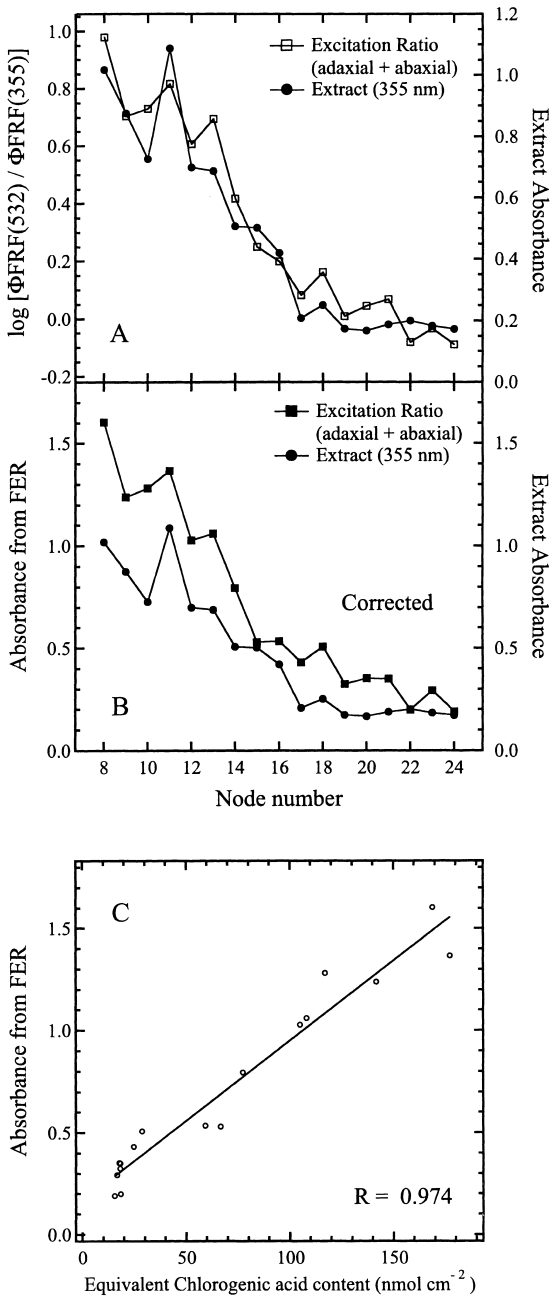

Fig. 9. Comparison of the estimated epidermal UV absorbance using the DE-FLIDAR and the UV absorbance of leaf extracts. The sum of the logarithm of the adaxial and abaxial FER is compared to the corresponding absorbance of extract, at 355 nm, (A) before and (B) after correction for the effect of Chl content by using the distortion function from Fig. 8B. (C) Comparison of the content of leaf phenolic compounds computed from the FER and from the maximum of absorbance of the extracts (326 nm). The phenolic content is expressed in equivalents of chlorogenic acid ($\varepsilon = 19000$ M^{-1} cm^{-1}).

we used total extracts of the leaf, containing the phenolic compounds of both the adaxial and abaxial epidermis (and even mesophyll), we compared the absorbance of extracts to the sum of the logarithm of the adaxial and abaxial FER. It can be seen that qualitatively equivalent estimation of UV-absorbing compounds was obtained by both methods. The content of UV-absorbing substances in the leaf epidermis is increasing with leaf age (smaller node number). The negative values of the logarithmic FER were mainly due to the abaxial leaf side. Indeed, on this side, the UV absorption of the epidermis is weak. Anyway, a relative comparison of epidermal UV absorbances using FER is possible, when the Chl content does not vary in a large range. In Fig. 9B, the same comparison is made but with FER corrected for the Chl effect using the distortion function. The corrected FER has a quantitative meaning, and can now be directly compared to extract absorbances (on the same numerical scale). The higher value for absorbance obtained by FER, compared to extracts, can be explained by the presence of UV-absorbing compounds bound to cell walls, not extractable by hot methanol. Still, the content of soluble UV-absorbing compounds is much larger than the ones bound to cell walls (Harris & Hartley, 1976; Lichtenthaler & Schweiger, 1998). Finally, in Fig. 9C, the corrected FER was plotted against the content of UV-absorbing compounds calculated using the maximal absorbance of the extracts (326 nm), and expressed as concentration of chlorogenic acid. This shows that after proper calibration, FER can be used to estimate quantitatively the content of UV-absorbing compounds in the leaf epidermis.

3.8. Changes in epidermal UV absorption during the development of pea canopies

Pea was chosen as a representative of dicotyledonous plants, for the analysis of the epidermal UV absorption at the canopy level. The measurements were performed, from the 4th day after seed imbibition to the 14th day of development on canopies grown indoors, in a growth cabinet, and outdoors, in July.

Fig. 10A shows the apparent FRF yield induced at 355 and 532 nm on indoor- and outdoor-grown pea canopies. Both canopies show an increasing green-induced ΦFRF(532) up to the 10th day, which corresponds to the full covering of the vermiculite trays (closed canopies). After the 10th day, the ΦFRF(532) remains constant. On the other hand, the UV-induced ΦFRF(355) increases over the whole growth period, for both indoor- and outdoor-

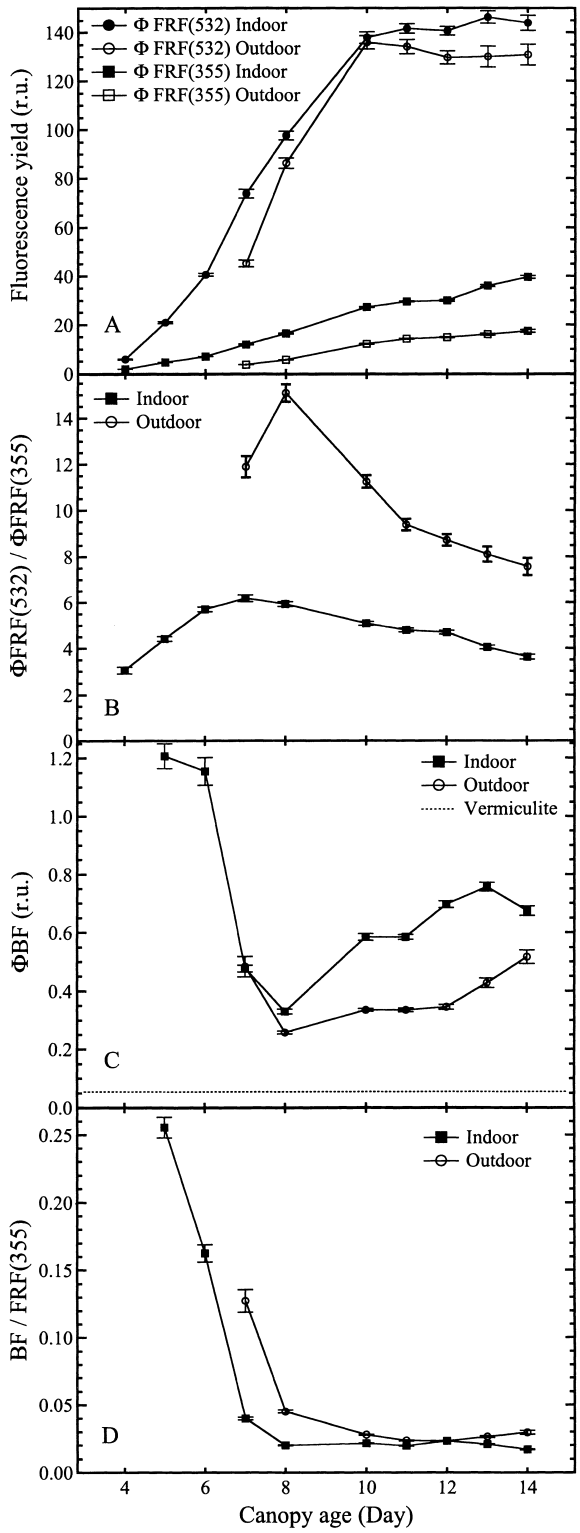

Fig. 10. Changes of FER and BF during the development of pea canopies. Fluorescence measurements were performed on pea canopies grown indoors, in a growth cabinet, and outdoors, in July, from day 4 after seed inhibition to day 14. (A) Apparent FRF yields, ΦFRF(532) and ΦFRF(355), excited at 532 and 355 nm, of indoor and outdoor grown pea canopies. (B) Changes of FER, ΦFRF(532)/ΦFRF(355), of pea canopies grown indoors and outdoors with time of development. (C) Changes in apparent BF yield, ΦBF, measured during the development of pea canopies. The dotted line at the bottom is the very low and constant signal obtained with pure wet vermiculite. The canopy temperature was maintained constant during the measurements at 20°C in order to avoid any effect on the BF. (D) BF to FRF(355) emission ratio, during the development of pea canopies. The error bars denote the standard deviation ($N = 170$).

grown canopies. Furthermore, both the UV and green-induced FRF were lower in pea grown outdoors under natural illumination containing UV radiation. Accordingly, the FER, ΦFRF(532)/ΦFRF(355), was always higher in outdoor-grown canopies (Fig. 10B). The FER is constantly changing during the development of both types of canopies, reaching a maximum value on the 7th and 8th day for indoor- and outdoor-grown canopies, respectively. The FER decreases thereafter.

We have shown already on tobacco leaves that FER is proportional to the epidermal UV absorption, or the reciprocal of UV transmittance: $T^{-1}(355)$. The differences in FER presented in Fig. 10B can therefore be interpreted as a consequence of a higher accumulation of UV-absorbing compounds in leaves of the canopy exposed to UV radiation. Indeed, an increase in UV-absorbing compounds in pea leaves was repeatedly reported upon exposure to UVB radiation (Day & Vogelmann, 1995; Gonzalez et al., 1996; He, Huang, Chow, Whitecross, & Anderson, 1993).

The interpretation of the changes in FER at the canopy level during the development is far more difficult. A canopy is a mixture of leaves of different ages and the soil coverage is constantly changing. For example, Gonzalez et al. (1996) reported a difference in the UV absorbance between bud tissue and mature pea leaves. The UV absorbance of extracts from buds was 50% lower than that of mature leaves. At an early stage of canopy development, pea buds predominate, with a low concentration of UV-absorbing compounds. Until the 7th day of development (cf. Fig. 10B), corresponding to the maximum value of the UV absorption, the buds were still closed and show the abaxial leaf side to the excitation beams (photographs were taken every day, not shown). After the 7th day, the leaves start to open and the canopy showed a complex structure with presence of a mixture of adaxial sides of old leaves and young closed leaves (abaxial side). Since pea plants initiate leaves at the rate of about one leaf every 2 days (Lyndon, 1977), the decreasing level of UV absorption of the canopy could be attributed to the presence of such young leaves which cover up the older ones.

A measurement of the BF was also performed concomitant to measurements of the FRF (Fig. 10C). Pure vermiculite was not fluorescent in the blue spectral range under our measuring conditions, and, therefore, it did not contribute to the BF signal. The canopy temperature was maintained constant during the measurements, at 20°C, in order to avoid any temperature dependency of the BF (Morales et al., 1998). At an early stage of development, pea seedlings showed a high BF yield (ΦBF), which correlated with a weak epidermal UV absorption (see Fig. 10C). ΦBF had a minimum value when the epidermal UV absorption was maximal and then, the BF increased as the FER decreased. Furthermore, after the 7th day, the outdoor-grown canopy always showed a lower BF than the indoor canopy. This antiparallel behaviour between BF and FER is readily explained by the mesophyll origin of BF in pea leaves. Cerovic et al. (1999) have shown that, in pea leaves, more than 40% of the BF originates from the mesophyll, thanks to the absence of ferulic acid from pea cell walls (Hartley & Harris, 1981). Apart from the constant BF coming from the cuticle (Hartley & Harris, 1981), the yield of BF in peas will be governed by the screening of mesophyll excitation. This is why the overall BF is increased when the UV screening by the epidermis is decreased (larger proportion of buds and abaxial sides seen by the DE-FLIDAR). This interpretation is corroborated by the smaller BF present in outdoor-grown canopies.

The often-used BF/FRF ratio (for a review, see Buschmann & Lichtenthaler, 1998) fails to differentiate outdoor- from indoor-grown plants. After the closing of the canopy, this ratio remains constant (see Fig. 10D). The initial decrease of the ratio during the first days of canopy development is principally due to BF decrease.

3.9. Changes in epidermal UV absorption during the development of barley canopies

The whole analysis performed on pea canopies was repeated on barley, which was chosen as a representative of monocotyledonous plants. Again, daily measurements were performed, on canopies grown indoors, in a growth cabinet, and outdoors, in July, from 4 to 14 days after planting. In Fig. 11, only the FER is shown for indoor- and outdoor-grown canopies. Both types of canopies showed an increasing FER with time of development, reaching a maximum, and then decreasing. Moreover, the barley grown outdoors showed a higher level of the FER, and, hence, a higher accumulation of UV-absorbing compounds, as

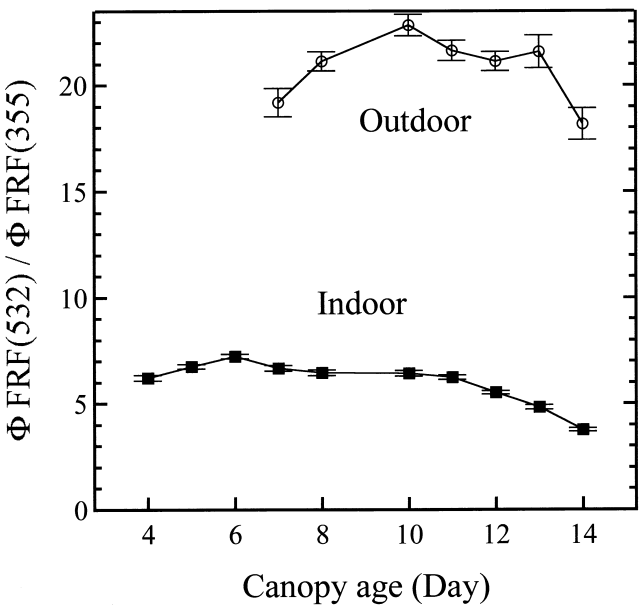

Fig. 11. Changes of FER during the development of barley canopies. FER measured from the 4th to the 14th day after planting. The barley canopies were grown indoors, in a growth cabinet, and outdoors, in July. The error bars denote the standard deviation ($N = 170$).

expected. Both flavonoids in the vacuole (Liu et al., 1995; Reuber et al., 1996) and phenolic acids, ferulic and *p*-coumaric, bound to the cell walls (Harris & Hartley, 1976) are known to be present in barley leaves. In addition, barley plants are reported to have about twice as much flavonoid per leaf when grown in presence of UVB radiation, and these relative levels are maintained throughout the life of the leaf (Liu et al., 1995). The differences between the indoor- and outdoor-grown canopies can easily be explained by the effect of UV radiation present in the natural illumination, but the interpretation of the changes with time is far subtler. As is typical for monocots, cells of barley leaves derive from a meristem located at the base of the leaf. Therefore, barley leaves have a gradient of younger tissue present at the base, and older tissue towards the tip (Tobin & Rogers, 1992). Hence, the decreasing level of the epidermal UV absorption of the canopy could be attributed to the increasing proportion of young cells seen by the DE-FLIDAR.

3.10. Comparison of epidermal UV absorption and BF among species and conditions of growth

Pea and barley canopies exhibit a weak difference in FER when grown indoors (Fig. 12). However, when grown under natural illumination, barley plant exhibits a much higher FER and, consequently, a higher epidermal UV absorption. Wheat canopies, another monocotyledonous plant of agronomic importance, were also tested. They showed a lower UV absorption than barley when grown outdoors.

Tobacco leaves grown indoors show a similar FER as pea and barley, when adaxial leaf sides are compared. By contrast, abaxial leaf sides of tobacco show much smaller FER. Therefore, by using the FER, it is easy to distinguish the adaxial from abaxial leaf side, and also to distinguish outdoor-grown from indoor-grown plants.

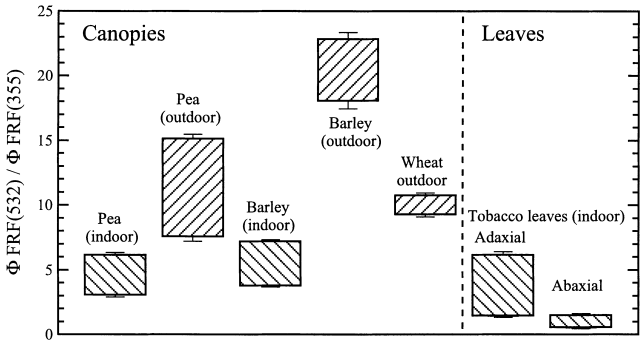

Fig. 12. Summary of observed FER for different plant species, grown indoors and outdoors. FER of different plant species, measured on single leaves (right side) and in a canopy structure (left side) is presented. Canopies of pea (*P. sativum* L., var. Petit Provençal) and barley (*H. vulgare*, cv Nevada) grown indoors, and canopies of pea, barley and wheat (*T. aestivum*, cv Lloyd) grown outdoors. FER of adaxial and abaxial sides of tobacco leaves (*N. tabacum*, cv Burley) grown indoors. For each species and growth conditions, the bar encompasses all the values of FER recorded, which depended on the stage of development. Left-oriented hatched bars indicate plants grown indoors and right-oriented hatched bars indicate plants grown outdoors. The error bars denote the standard deviation ($N = 170$).

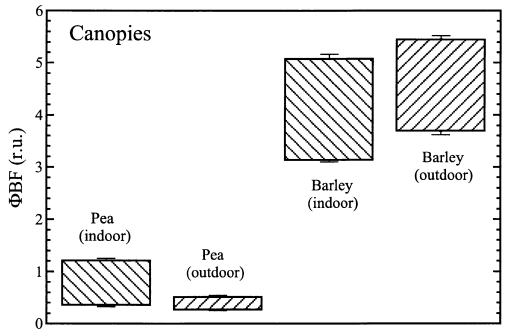

Fig. 13. Summary of observed BF yield of pea (*P. sativum* L., var. Petit Provençal) and barley (*H. vulgare*, cv Nevada) canopies, grown under the same conditions, in a growth cabinet, and outdoors, in July. For each species and growth conditions, the bar encompasses all the values of BF recorded, which depended on the stage of development. Left-oriented hatched bars indicate plants grown indoors and right-oriented hatched bars indicate plants grown outdoors. The error bars denote the standard deviation ($N = 170$).

Fig. 13 shows a comparison between the BF yield of pea and barley canopies, grown indoors and outdoors. As expected for monocotyledonous plants, which exhibit a much higher BF emission than leaves of dicotyledonous plants (Lichtenthaler & Schweiger, 1998), barley canopies had a higher BF than pea canopies. When grown outdoors, barley canopy exhibited a weak increase in BF compared to indoor conditions. Pea canopies showed a much higher decrease in BF when grown outdoors. This is due to a different origin of BF in barley and pea, as explained above (cf. Cerovic et al., 1999).

4. Concluding remarks

The DE-FLIDAR presented in this report is based on a dual-wavelength excitation and multiwavelength emission. The main new signature available with this FLIDAR: the FER, ΦF(532)/ΦF(355), was shown to be insensitive to variable ChlF and to the angle of incidence of the excitation. We showed both theoretically and experimentally that the logarithm of FER corresponds to the UV absorbance of the leaf epidermis at 355 nm. Yet, one has to take into account the distortion effect due to the variable Chl content among leaves, which can affect this signature. On the other hand, we also showed that quantitative measurements, without correction for the Chl content, could be performed if the ChlF is measured in the red part of the emission spectrum, as RF instead of FRF. Indeed, the distortion function $D(C_{Chl}, \lambda_{em})$, in this case, exhibits a relatively constant offset of 0.5 for a Chl content above 20 μg cm^{-2}, which is generally the case for most adult leaves.

In addition, our model showed that the excitation ratio is not dependent on the leaf Chl content when the absorptiv-

ities of the Chl are identical at the UV and reference excitation wavelengths. The actual DE-FLIDAR does not fulfil this condition, because it uses the harmonic frequencies of a Nd:YAG laser. However, on the other hand, the use of a reference wavelength close to the minimum of absorption of Chl (532 nm) enables the estimation of the leaf Chl content with the DE-FLIDAR. Indeed, a dual RF to FRF emission ratio, excited at 355 and 532 nm, "[RF(355)/FRF(355)]/[RF(532)/FRF(532)]" was shown to be linearly dependent on the Chl content.

The epidermal UV absorption, estimated using the DE-FLIDAR, was shown to vary over a wide range for different plant species (tobacco, pea, barley). The FER was much larger in outdoor-grown plants, as expected, indicating an accumulation of UV-absorbing compounds. Indeed, the leaf epidermis is screening and protecting the mesophyll against UV radiation, and this effect is very much dependent on the irradiance under which the leaf has grown. Furthermore, with this FLIDAR, estimation of epidermal UV absorption can be coupled to the measurement of blue-green fluorescence and leaf Chl content to provide more complete information for plant identification (monocots vs. dicots and sun plants vs. shade plants), and for the monitoring of plant growth and development, presence of mineral deficiency or other stress conditions.

Acknowledgments

We would like to acknowledge the support of the CNRS through the GDR 1536 "FLUOVEG". During this work, A.O. was supported by a grant from the "Société de Secours des Amis de Sciences", Paris, France. The authors wish to thank G. Latouche for the help with measurements of fluorescence spectra, Y. Goulas for a critical examination of the model and a comparison to the Kubelka–Munk theory and Y. le Breton (ITCF) for providing cereal seeds.

References

Agati, G., Fusi, F., Mazzinghi, P., & diPaola, M. L. (1993). A simple approach to the evaluation of the reabsorption of chlorophyll fluorescence spectra in intact leaves. *Journal of Photochemistry and Photobiology, B: Biology*, *17*, 163–171.

Anderson, M., Edner, H., Johansson, J., Ragnarson, P., Svanberg, S., & Wallinder, E. (1994). Remote monitoring of vegetation by spectral measurements and multi-colour fluorescence imaging. In: G. Guyot (Ed.), *Physical measurements and signatures in remote sensing* (pp. 835–842). Val d'Isère, France: CNES.

Bate-Smith, E. C. (1962). The phenolic constituents of plants and their taxonomic significance. *Journal of the Linnean Society of London, Botany*, *58*, 95–175.

Bilger, W., Veit, M., Schreiber, L., & Schreiber, U. (1997). Measurement of leaf epidermal transmittance of UV radiation by chlorophyll fluorescence. *Physiologia Plantarum*, *101*, 754–763.

Bornman, J. F., & Vogelmann, T. C. (1988). Penetration of blue and UV radiation measured by fiber optics in spruce and fir needles. *Physiologia Plantarum*, *72*, 699–705.

Bruinsma, J. (1961). A comment on the spectrophotometric determination of chlorophyll. *Biochimica et Biophysica Acta*, *52*, 576–578.

Buschmann, C., & Lichtenthaler, H. K. (1998). Principles and characteristics of multi-colour fluorescence imaging of plants. *Journal of Plant Physiology*, *152*, 297–314.

Caldwell, M. M. (1971). Solar UV irradiation and the growth and development of higher plants. In: A. C. Giese (Ed.), *Photophysiology* (pp. 131–171). New York: Academic Press.

Caldwell, M. M., Bjorn, L. O., Bornman, J. F., Flint, S. D., Kulandaivelu, G., Teramura, A. H., & Tevini, M. (1998). Effects of increased solar ultraviolet radiation on terrestrial ecosystems. *Journal of Photochemistry and Photobiology, B: Biology*, *46*, 40–52.

Caldwell, M. M., Robberecht, R., & Flint, S. D. (1983). Internal filters: prospects for UV-acclimation in higher plants. *Physiologia Plantarum*, *58*, 445–450.

Cecchi, G., Mazzinghi, P., Pantani, L., Valentini, R., Tirelli, D., & De Angelis, P. (1994). Remote sensing of chlorophyll a fluorescence of vegetation canopies: 1. Near and far field measurement techniques. *Remote Sensing of Environment*, *47*, 18–28.

Cecchi, G., Pantani, L., Bazzani, M., Raimondi, V., Mazzinghi, P., & Valentini, R. (1994). Lidar remote sensing of vegetation status: the link to plant physiology. In: C. Werner, & W. Waidelich (Eds.), *Laser in remote sensing* (pp. 75–77). Berlin: Springer.

Cerovic, Z. G., Bergher, M., Goulas, Y., Tosti, S., & Moya, I. (1993). Simultaneous measurement of changes in red and blue fluorescence in illuminated isolated chloroplasts and leaf pieces: the contribution of NADPH to the blue fluorescence signal. *Photosynthesis Research*, *36*, 193–204.

Cerovic, Z. G., Cheesbrough, J. K., & Walker, D. A. (1987). Photosynthesis by intact isolated chloroplasts on solid support. *Plant Physiology*, *84*, 1249–1251.

Cerovic, Z. G., Goulas, Y., Gorbunov, M., Briantais, J.-M., Camenen, L., & Moya, I. (1996). Fluorosensing of water stress in plants. Diurnal changes of the mean lifetime an yield of chlorophyll fluorescence, measured simultaneously and at distance with a τ-LIDAR and a modified PAM-fluorimeter, in maize, sugar beet and Kalanchoë. *Remote Sensing of Environment*, *58*, 311–321.

Cerovic, Z. G., Langrand, E., Latouche, G., Morales, F., & Moya, I. (1998). Spectral characterization of NAD(P)H fluorescence in intact isolated chloroplasts and leaves: effect of chlorophyll concentration on reabsorption of blue-green fluorescence. *Photosynthesis Research*, *56*, 291–301.

Cerovic, Z. G., & Plesnicar, M. (1984). An improved procedure for the isolation of intact chloroplasts of high photosynthetic capacity. *Biochemical Journal*, *223*, 543–545.

Cerovic, Z. G., Samson, G., Morales, F., Tremblay, N., & Moya, I. (1999). Ultraviolet-induced fluorescence for plant monitoring: present state and prospects. *Agronomie: Agriculture and Environment*, *19*, 543–578.

Chekalyuk, A. M., & Gorbunov, M. Y. (1995). Development of the lidar pump-and-probe technique for remote measuring the efficiency of primary photochemical reactions in leaves of green plants. *EARSeL Advanced Remote Sensing*, *3*, 42–56.

Cui, M., Vogelmann, T. C., & Smith, W. K. (1991). Chlorophyll and light gradients in sun and shade leaves of *Spinacia oleracea*. *Plant and Cell Environment*, *14*, 493–500.

Day, T. A., Howells, B. W., & Rice, W. J. (1994). Ultraviolet absorption and epidermal-transmittance spectra in foliage. *Physiologia Plantarum*, *92*, 207–218.

Day, T. A., & Vogelmann, T. C. (1995). Alterations in photosynthesis and pigment distributions in pea leaves following UV-B exposure. *Physiologia Plantarum*, *94*, 433–440.

del Moral, R. (1972). On the variability of chlorogenic acid concentration. *Oecologia*, *9*, 289–300.

Edner, H., Johansson, J., Svanberg, S., & Wallinder, E. (1994). Fluorescence lidar multicolor imaging of vegetation. *Applied Optics*, *33*, 2471–2479.

Fukshansky, L., & Kazarinova, N. (1980). Extension of the Kubelka–Munk theory of light propagation in intensely scattering materials to fluorescence media. *Journal of the Optical Society of America*, *70*, 1101–1111.

Gausman, H. W., Rodriguez, R. R., & Escobar, D. E. (1975). Ultraviolet radiation reflectance, transmittance, and absorptance by leaf epidermises. *Agronomy Journal*, *67*, 720–724.

Gonzalez, R., Paul, N. D., Percy, K., Ambrose, M., McLaughlin, C. K., Barnes, J. D., Areses, M., & Wellburn, A. R. (1996). Responses to ultraviolet-B radiation (280–315 nm) of pea (*Pisum sativum*) lines differing in leaf surface wax. *Physiologia Plantarum*, *98*, 852–860.

Goulas, Y., Camenen, L., Briantais, J.-M., Schmuck, G., Moya, I., & Guyot, G. (1994). Measurements of laser-induced fluorescence decay and reflectance of plant canopies. In: G. Guyot (Ed.), *Physical measurements and signatures in remote sensing* (pp. 937–944). Val d'Isère, France: CNES.

Günther, K. P., Lüdeker, W., & Dahn, H.-G. (1991). Design and testing of a spectral-resolving fluorescence LIDAR system for remote sensing of vegetation. In: J. J. Hunt (Ed.), *Proceedings of the 5th international colloquium of physical measurements and signatures in remote sensing* (pp. 723–726). Courchevel, France: ESA (SP-319).

Harris, P. J., & Hartley, R. D. (1976). Detection of bound ferulic acid in the cell walls of the Gramineae by ultraviolet fluorescence microscopy. *Nature*, *259*, 508–510.

Hartley, R., & Harris, P. (1981). Phenolic constituents of the cell walls of dicotyledons. *Biochemical Systematics and Ecology*, *9*, 189–203.

He, J., Huang, L. K., Chow, W. S., Whitecross, M. I., & Anderson, J. M. (1993). Effect of supplementary ultraviolet-B radiation on rice and pea plants. *Australian Journal of Plant Physiology*, *20*, 129–142.

Hoge, F. E., Swift, R. N., & Yungel, J. K. (1983). Feasibility of airborne detection of laser induced emissions from green terrestrial plants. *Applied Optics*, *22*, 2991–3000.

Koeppe, D. E., Rohrbaugh, L. M., & Wender, S. W. (1969). The effect of varying UV intensities on the concentration of scopolin and caffeoylquinic acids in tobacco and sunflower. *Phytochemistry*, *8*, 889–896.

Lautenschlager-Fleury, D. (1955). Uber die Ultraviolettdurshlässigkeit von Blattepidermien. *Berichte der Schweizerischen Botanischen Gesellschaft*, *65*, 343–386.

Lichtenthaler, H. (1987). Chlorophylls and carotenoids: pigments of photosynthetic membranes. *Methods in Enzymology*, *148*, 350–382.

Lichtenthaler, H. K., & Rinderle, U. (1988). The role of chlorophyll fluorescence in the detection of stress conditions in plants. *CRC Crititical Reviews in Analytical Chemistry*, *19*, 29–85.

Lichtenthaler, H. K., & Schweiger, J. (1998). Cell wall bound ferulic acid, the major substance of the blue-green fluorescence emission of plants. *Journal of Plant Physiology*, *152*, 272–282.

Lichtenthaler, H. K., Stober, F., Buschmann, C., Rinderle, U., & Hak, R. (1990). Laser-induced chlorophyll fluorescence and blue fluorescence of plants. In: *International Geoscience and Remote Sensing Symposium, IGARSS '90, Washington, DC* (pp. 1913–1918). College Park: University of Maryland.

Liu, L., Gitz, D. C. III, & McClure, J. W. (1995). Effects of UV-B on flavonoids, ferulic acid, growth and photosynthesis in barley primary leaves. *Physiologia Plantarum*, *93*, 725–733.

Loche, J., & Chouteau, J. (1963). Incidence des carences en Ca, Mg ou P sur l'accumulation des polyphénols dans la feuille de tabac. *Comptes Rendus de l'Academie d'Agriculture de France*, *49*, 1017–1026.

Lyndon, R. F. (1977). The shoot apical meristem. In: J. F. Sutcliffe, & J. S. Pate (Eds.), *The physiology of the garden pea* (pp. 183–211). London: Academic Press.

Middleton, E. M., Chappelle, E. W., Cannon, T. A., Adamse, P., & Britz, S. J. (1996). Initial assessment of physiological response to UV-B irradiation using fluorescence measurements. *Journal of Plant Physiology*, *148*, 69–77.

Morales, F., Cerovic, Z. G., & Moya, I. (1998). Time-resolved blue-green fluorescence of sugar beet leave. Temperature-induced changes and consequences for the potential use of blue-green fluorescence as a signature for remote sensing of plants. *Australian Journal of Plant Physiology*, *25*, 325–334.

Moya, I., Goulas, Y., Morales, F., Camenen, L., Guyot, G., & Schmuck, G. (1995). Remote sensing of time-resolved chlorophyll fluorescence and back-scattering of the laser excitation by vegetation. *EARSeL Advanced Remote Sensing*, *3*, 188–197.

Percival, M. P., & Baker, N. R. (1985). Comparison of chlorophyll fluorescence emission characteristics of wheat leaf tissue and isolated thylakoids as a function of excitation wavelength. *Plant and Cell Environment*, *8*, 41–48.

Reuber, S., Bornman, J. F., & Weissenbock, G. (1996). A flavonoid mutant of barley (*Hordeum vulgare* L.) exhibits increased sensitivity to UV-B radiation in the primary leaf. *Plant and Cell Environment*, *19*, 593–601.

Rosema, A., Cecchi, G., Pantani, L., Radicatti, B., Romuli, M., Mazzinghi, P., Van Kooten, O., & Kliffen, C. (1988). Results of the 'LIFT' project: air pollution effects on the fluorescence of douglas fir and poplar. In: H. K. Lichtenthaler (Ed.), *Applications of chlorophyll fluorescence* (pp. 306–317). Netherlands: Kluwer Academic Publishers.

Sandhu, R., Kim, M. S., Krizek, D. T., & Middleton, E. (1997). Fluorescence imaging and chlorophyll fluorescence to evaluate the role of EDU in UV-B protection in cucumber. In: *Aerosense '97* (pp. 42–50). Bellingham, SPIE.

Schnitzler, J.-P., Jungblut, T. P., Heller, W., Köfferlein, M., Hutzler, P., Heinzmann, U., Schmelzer, E., Ernst, D., Langebartels, C., & Sandermann, H. J. (1996). Tissue localization of UV-B screening pigments and of chalcone synthase mRNA in Scots pine (*Pinus silvestris* L.) needles. *New Phytologist*, *132*, 247–258.

Schweiger, J., Lang, M., & Lichtenthaler, H. K. (1996). Differences in fluorescence excitation spectra of leaves between stressed and non-stressed plants. *Journal of Plant Physiology*, *148*, 536–547.

Sheahan, J. J. (1996). Sinapate esters provide greater UV-B attenuation than flavonoids in *Arabidopsis thaliana* (Brassicaceae). *American Journal of Botany*, *83*, 679–686.

Stober, F., & Lichtenthaler, H. K. (1993). Characterization of the laser-induced blue, green and red fluorescence signatures of leaves of wheat and soybean grown under different irradiance. *Physiologia Plantarum*, *88*, 696–704.

Takahama, U. (1998). Ascorbic acid-dependent regulation of redox levels of chlorogenic acid and its isomers in the apoplast of leaves of *Nicotiana tabacum* L. *Plant and Cell Physiology*, *39*, 681–689.

Teramura, A. H., & Sullivan, J. H. (1994). Effects of UV-B radiation on photosynthesis and growth of terrestrial plants. *Photosynthesis Research*, *39*, 463–473.

Tevini, M., & Teramura, A. H. (1989). UV-B effects on terrestrial plants. *Photochemistry and Photobiology*, *50*, 479–487.

Tobin, A. K., & Rogers, W. J. (1992). Plant organelles. Compartmentation of metabolism in photosynthetic cells. In: A. K. Tobin (Ed.), *Plant organelles: compartmentation of metabolism in photosynthetic cells* (pp. 293–323). Cambridge: Cambridge Univ. Press.

Vogelmann, T. C. (1993). Plant tissue optics. *Annual Review of Plant Physiology and Plant Molecular Biology*, *44*, 231–251.